Irradiance forecast model for PV generation based on cloudiness web service

Irradiance forecast model for PV generation based on cloudiness web service

Dung V Nguyen[1,2], Benoit Delinchant[1*], Binh V Dinh[1] and Truong X Nguyen[2]

1 Univ. Grenoble Alpes, CNRS, Grenoble INP, G2Elab, 38000 Grenoble, France
2 University of Science and Technology of Hanoi, Hanoi, Vietnam
*E-mail: benoit.delinchant@G2Elab.grenoble-inp.fr

Abstract. Among renewable energies that play a critically important role to achieve a sustainable development in the future, solar photovoltaic (PV) power have been growing dramatically recently. Despite the enormous potential of solar PV, its drawback, which is intermittent in generation, imposes a significant issue on electrical system, such as stability or operation planning of the system. One of the solutions for the problem is PV generation forecast that have been researched in various studies. This paper presents a methodology to obtain an indirect PV production forecast model. Processes of model formation, validation and test are performed in the study using real data from a Campbell Scientific weather station Grenoble, France.

1. Introduction

In this paper, we are focusing on hourly electricity power generated by photovoltaic panels from solar irradiance. There are two major categories of PV power forecasting models, which are indirect and direct forecasting model. Direct forecasting models gives directly PV production as a result. Whereas, in the indirect forecasting models, solar irradiance is forecasted then PV production is derived based on the amount of irradiance.

Our PV production forecast modelling methodology has two steps: firstly, an irradiance forecast model is created based on empirical formula and data; secondly, predicted irradiances are applied in an indirect PV production model. In this paper only the first step is detailed.

Solar irradiance can be decomposed in Direct Normal Irradiance (DNI, in W/m^2) and Global Horizontal Irradiance (GHI, in W/m^2). These two components can be measured using a Rotating Shadowband Radiometer available in our weather station in Grenoble, France. Our methodology requires also a cloudiness forecast which can be available using weather services available on the Internet (free or not).

In this paper, 8 models of clear sky irradiance are compared and one is chosen to be used in our methodology. From this model and cloudiness forecast, we are proposing models to forecast real GHI and DNI which are then compared to two models available in the literature.

At the end of the paper, the forecast is also compared to real measures in order to validate it in a short term horizon (hours) and a long term horizon (days). The irradiance difference is analysed regarding weather forecast accuracy, and the error regarding energy production is also analysed.

2. Modelling methodology

2.1. Photovoltaic production model

Hourly electricity power generated by photovoltaic panels from solar irradiance can be given by the following model:

$$P_{PV}(t) = \eta_{PV}.S_{PV}.POA(t) \quad (2\text{-}1)$$

S_{PV} is the PV area (m^2);
η_{PV} is the system global efficiency which is calculated from the producer's reference efficiency n_{ref} (at the standard condition: 25 ℃, 1000W/m2), real efficiency n_{real} (taking into account losses due to temperature, radiation level, connection loss, wiring loss etc) and inverter efficiency $n_{inverter}$

$$\eta_{PV} = \eta_{ref}.\eta_{real}.\eta_{inverter} \quad (2\text{-}2)$$

Typical values are $n_{ref} = 0.2$ for polycrystalline modules, $n_{real} = 0.8$, and $n_{inverter} = 0.95$. It is leading to a typical efficiency of 15%. This study is not focused on modeling the efficiency.
The last term of equation (2-1) is $POA(t)$ which represents the global solar irradiance on the panel plane (W/m^2), which is composed of 3 components (direct, diffuse and reflection) and is derived from the weather data of Direct Normal Irradiance (DNI, in W/m^2) and Global Horizontal Irradiance (GHI, in W/m^2) using geometric considerations that are not detailed here (more information for instance on Sandia web site[1]).

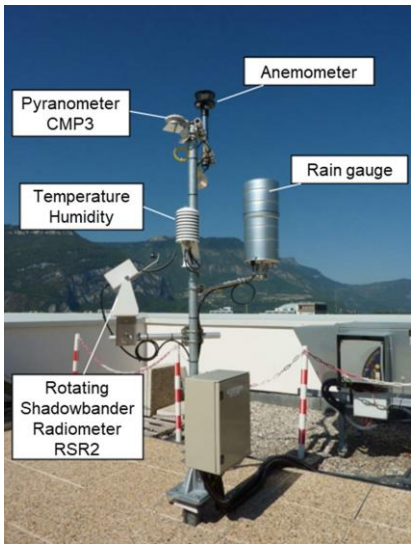

Figure 1. weather station meteo-greener.g2elab.grenoble-inp.fr

2.2. Measuring irradiances
It is then possible to obtain the PV production using this model and measures of DNI and GHI. These irradiances are obtained in this study using the Rotating Shadowband Radiometer of our weather station (**Figure 1**). More information in such a scientific instrument in [1].

2.3. Forecasting irradiances
Our aim is to forecast PV production at the horizon of 24h, the day ahead. To do this, it is proposed in this paper to focus on irradiances forecasting.
An important information on solar irradiance is the sky cloud cover, or cloudiness. It is now possible to obtain cloudiness forecast from weather forecast web services such as AROME model from Meteo-France[2] which is a small scale numerical prediction model, designed to improve short range forecasts. The term *cloudiness* in this study is used to describe the percentage that the cloud covers the sky. In some studies, it can be *cloud cover*, however *cloud cover* can be referred to how many octas of the sky that is covered, where an octa corresponds to a fraction of $1/8^{th}$ of the celestial vault.
There is already empirical model on solar radiation forecast that set cloudiness as an input, one of first studies [2] established the relationship as in equation (2-3):

$$\frac{GHI(N)}{GHI(0)} = 1 - 0.75 \times \left(\frac{N}{8}\right)^{3.4} \quad (2\text{-}3)$$

Where: $GHI(N)$ is Global Horizontal Irradiance at N octas, $GHI(0)$ is clear-sky GHI.
In another study [3], equation(2-4) and(2-5) were proposed to compute solar radiation based on cloud cover and clear-sky irradiance models.

$$DNI = DNI_{clear} \times K \times \left(1 - \frac{CC}{10}\right) \quad (2\text{-}4)$$

[1] https://pvpmc.sandia.gov/modeling-steps/1-weather-design-inputs/plane-of-array-poa-irradiance/
[2] https://www.umr-cnrm.fr/spip.php?article120&lang=en

$$DHI = DHI_{clear} \times \left(CCF - K \times \left(1 - \frac{CC}{10} \right) \right) \quad (2\text{-}5)$$

Where: DNI is Direct Normal Irradiance, DNI_{clear} is clear-sky direct normal irradiance, K is cloud cover modifier, CC is cloud cover measured out of 10. DHI is Diffuse Horizontal Irradiance, DHI_{clear} is clear-sky diffuse horizontal irradiance, CCF = 1.028 + 0.0195 CC + 0.0095 CC^2.

Kasten and Czeplak relationship in 1980 was then improved to optimize for a case study with the weather condition in the US [4] as equation(2-6) :

$$\frac{GHI(N)}{GHI(0)} = 1 - 0.87 \times \left(\frac{N}{8} \right)^{1.9} \quad (2\text{-}6)$$

Further complex models are available in [5], [6], yet they are always optimal for the target regions of research. In this study, a correlation between cloudiness and solar irradiance will be constructed, based on cloudiness forecast and clear-sky irradiance, in order to have forecast of incidence irradiance to the PV as in equation (2-1).

There are many clear-sky irradiance models proposed through years, therefore in order to analyse them easily, they will be classified into three groups of very simple, simple and complex models. The first group is very simple models, in which only geometric calculation is considered [7]–[16].

The second group contains simple models, in which additional basic parameters that describe a state of the atmosphere are included like air pressure, temperature, relative humidity, elevation, Linke turbidity [17]–[19].

The last group consists of complex models, where various atmospheric variables are considered such as ozone, perceptible water or aerosols. These kinds of models reach the highest accuracy if required parameters are measured properly, however, they are not always available. List of complex models are not listed here due to their complexity but they can be found in these review journals [13], [15], [20].

2.4. Methodology

We are now proposing a methodology in order to forecast PV production. Past values of measured irradiances associated with a clear-sky irradiance model can be correlated with cloudiness forecast history (**Figure 2**) to create our irradiance forecasting model. This model will be used to predict irradiances based on forecasted cloudiness, then Hay transposition model [21] will be applied to obtain forecasted PV production (**Figure 3**). This methodology is detailed and applied in the following sections.

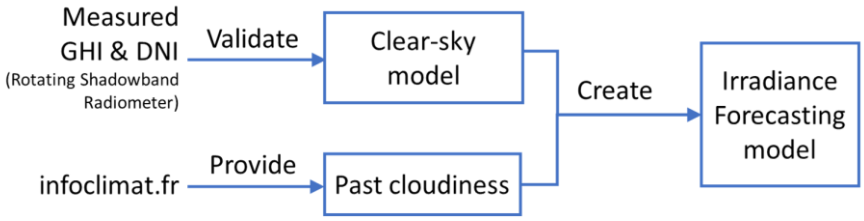

Figure 2: Methodology to create irradiance forecasting model

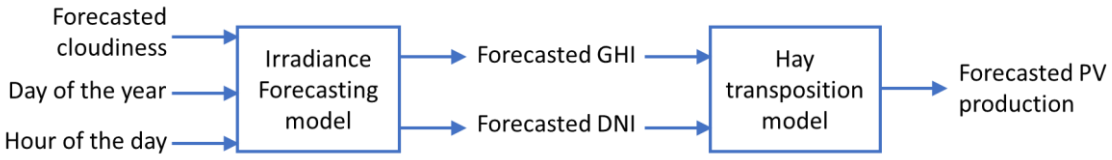

Figure 3: PV forecasting

3. Irradiance forecast models

3.1. Clear-sky model validation

There is no universal model developed yet, therefore it is not clear about what clear sky irradiance model can be applied for a specific area unless the model is constructed in the region. The largest discrepancy between models' results were found when the models are applied over great aerosol loads, drastically high or low water vapor content areas [15, p. 26].
Our model is intended to be used with a minimal set of available weather forecast (only cloudiness), then only very simple (Table 1) and simple clear-sky models are considered (Table 2).

Table 1: The first group is very simple models

Daneshyar–Paltridge–Proctor [7], [8] *z is zenith angle of the sun*	$DNI = 950.2 \times \left(1 - e^{-0.075\times(90°-z)}\right)$ $DHI = 14.29 + 21.04 \times \left(\frac{\pi}{2} - z \times \frac{\pi}{180}\right)$ $GHI = DNI \times \cos(z) + DHI$
Kasten–Czeplak (KC) [2]:	$GHI = 910 \times \cos(z) - 30$
Haurwitz [9], [16]	$GHI = 1098 \times \cos(z) \times e^{\frac{-0.057}{\cos(z)}}$
Berger–Duffie (BD) [10]:	$GHI = I_o \times 0.7 \times \cos(z)$
Adnot–Bourges–Campana–Gicquel [11]	$GHI = 951.39 \times \cos(z)^{1.15}$
Robledo-Soler (RS) [12]:	$GHI = 1159.24 \times \cos(z)^{1.179} \times e^{-0.0019\times(90°-z)}$
Meinel Model [13]	$DNI = I_o \times 0.7^{AM^{0.678}}$ *(AM: air mass)*
Laue Model [14]	$DNI = I_o \times ((1 - 0.14 \times h) \times 0.7^{AM^{0.678}} + 0.14 \times h)$ *I_o is the extra-terrestrial radiation, h is elevation*

Table 2: The second group is simple models

Hottel [17]	$DNI = I_o \times \left(a_0 + a_1 \times e^{\frac{-k}{\cos(z)}}\right)$
Kasten [18] *TL is Linke Turbidity*	$GHI = 0.84 \times I_o \times \cos(z) \times e^{\left(-0.027\times AM\times\left(f_{h1} + f_{h2}\times(TL-1)\right)\right)}$
Ineichen and Perez [19]:	$GHI = c_{g1} \times I_o \times \cos(z) \times e^{\left(-c_{g2}\times AM\times\left(f_{h1} + f_{h2}\times(TL-1)\right)\right)}$

These models are compared in Figure 4. The result is that model from Adnot–Bourges–Campana–Gicquel [11] is the best candidate for our clear-sky GHI model.

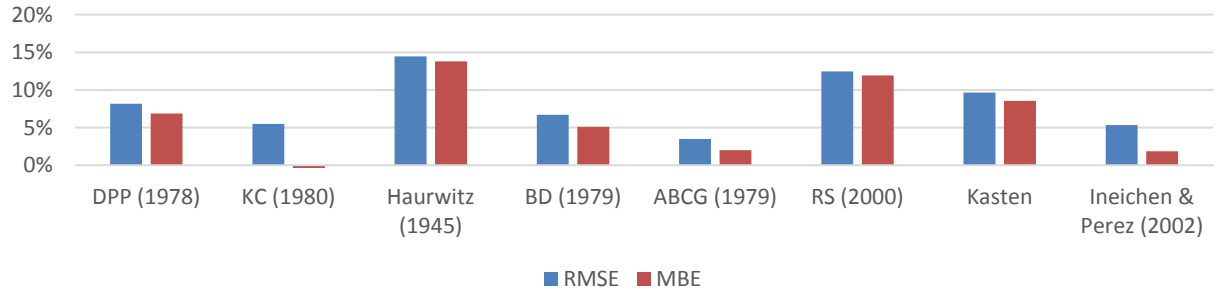

Figure 4. Root Mean Square Error (RMSE) and Mean Bias Error (MBE) of clear sky irradiance

3.2. Irradiance model creation

On the next parts, only GHI analysis is presented. The same procedure is applied to DNI.

During model creation process, the data used is a set of cloudiness records in July and August 2018. Each record is taken from the weather web service (infoclimat.fr) at the current time. It means that cloudiness at 11:00 in our records has been taken from the web site at 11:00. The accuracy is then maximal, it is not a long term forecast. Each value has been saved to create our database.
Figure 5 is a box plot (minimum, first quartile, median, third quartile, and maximum) of the ratio of measured GHI over clear-sky GHI (GHI/GHI_0) depending on cloudiness.
The mean value of box plot is showing that cloudiness is not influencing a lot before 80% with a ratio that is slowly decreasing but leading to value above 0.8. When the sky is overcast (the cloudiness>95%), GHI/GHI_0 ratio has the mean distribution value around 0.4. The main reason is diffuse irradiance that reflects through layers of cloud.
In order to build a regression model from these data, the hypothesis of Kasten and Czeplak [2] is made as defined in equation (3-1):

$$\frac{measured\ GHI}{clear\ sky\ GHI} = 1 - a \times cloudiness^{\,n} \tag{3-1}$$

Coefficients *a* and *n*, are obtained to fit the weather condition in Grenoble, using Nelder-Mead optimization method. The values obtained are a=0.51 and n=6.42, and the corresponding regression is the red continuous line in **Figure 5**

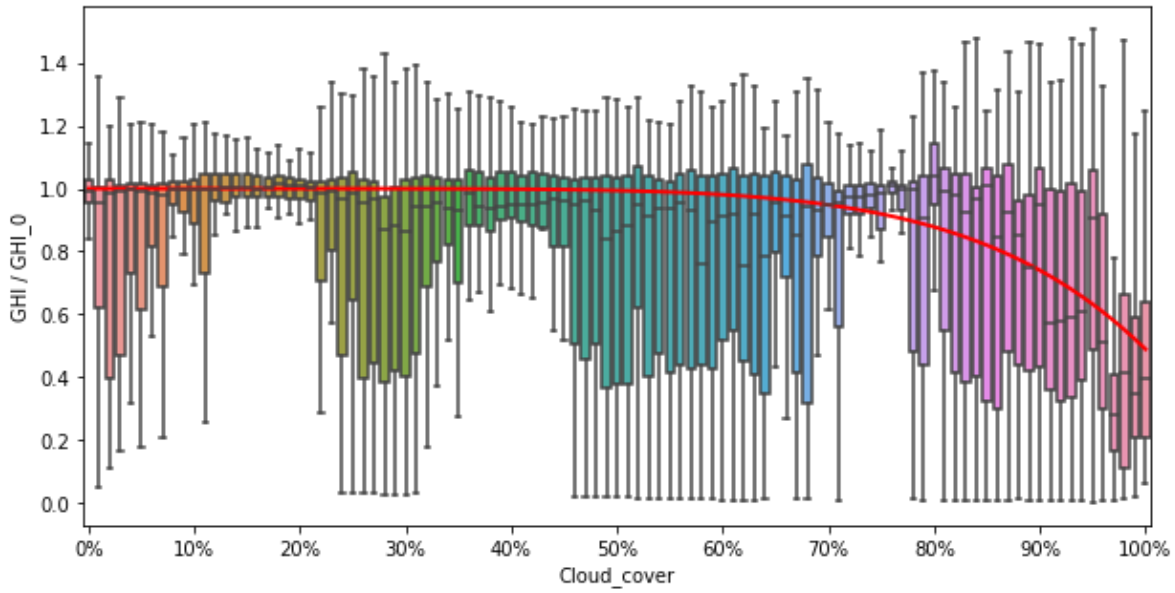

Figure 5. Boxplot distribution of ratio measured GHI over clear-sky GHI (GHI_0) corresponding to cloudiness in July and August. The red line's equation is $y = 1 - 0.51 \times x^{6.42}$

3.3. Model comparison
In this section, our model is compared with Perez model [4] and Kasten and Czeplak (KC) [2] using past cloudiness value for a half of September 2018. This data set was recorded in the same manner as past cloudiness data in July and August 2018 during the model creation process.
Figure 6 is the violin plot of these 3 models. In the heart of the plot is a box plot, in which the white dot is the median, the box is interquartile range, and the rod is 95% confidence interval. Outside part is Kernel density estimation (KDE) plot of the error distribution. In all three plots, the highest density of error is around -100 to 100 W/m^2.

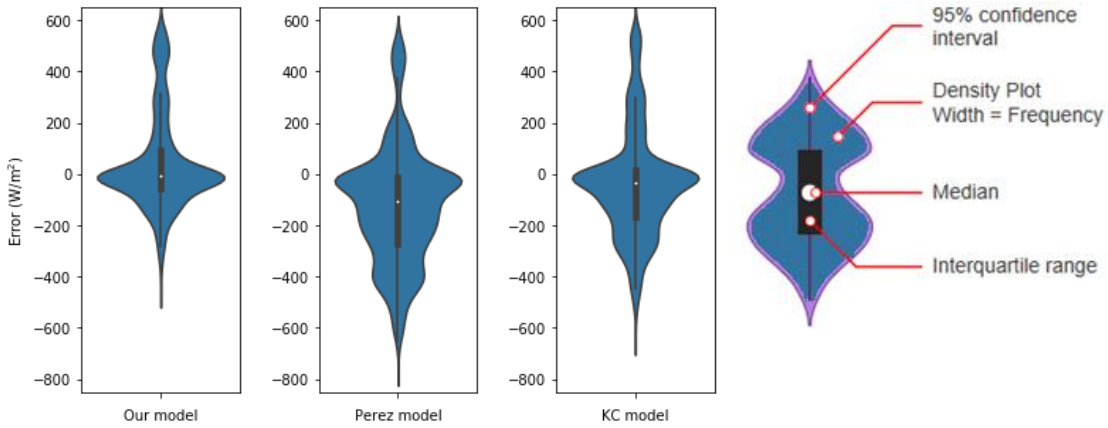

Figure 6. Error distribution of three models

As it can be seen more clearly in **Table 3**, which compares the error between the calculated GHI and measured GHI, the median and mean of error by our model in this study are closest to zero, and its standard deviation is smallest. Furthermore, the root mean square error (RMSE) in this study is 194 while those in Perez study and KC study are 256 and 211 respectively. Therefore, the model in this study is more reliable and suitable in our context.

Table 3: Detailed parameters of the error distribution

Error distribution	**Our model**	**Perez model**	**KC model**
Median (W/m^2)	-16.1	-66.4	-34.4
Mean (W/m^2)	29.9	-110.3	-38.4
Standard deviation (W/m^2)	170.7	202.3	186.2

3.4. Irradiance model forecast validation

The dataset used for model test is three-hour forecasted cloudiness in September 2018. For instance, the cloudiness value in the dataset at 11:00 is recorded 3 hours earlier at 8:00. In order to ensure accuracy of evaluation, only daily data when the sun is available is used during analysis.

As demonstrated in **Figure 7**(a), the correlation between forecasted GHI and measured GHI is quiet good for lot of samples, even with a coefficient of determination r^2 equal to 0.58. The error distribution is presented in **Figure 7**(b), where the median and mean are quite close to zero, with value of 3.41 W/m^2 and 36.25 W/m^2 respectively, while standard deviation is 140.3 W/m^2. As shown in the violin plot, 95% of error ranges are from -120 W/m^2 to 155 W/m^2, and 50% of error are from -15 W/m^2 to 50 W/m^2. There are some outliers with big error because there was a day when cloudiness forecast was totally wrong (forecasted a clear sky, but cloudy in reality).

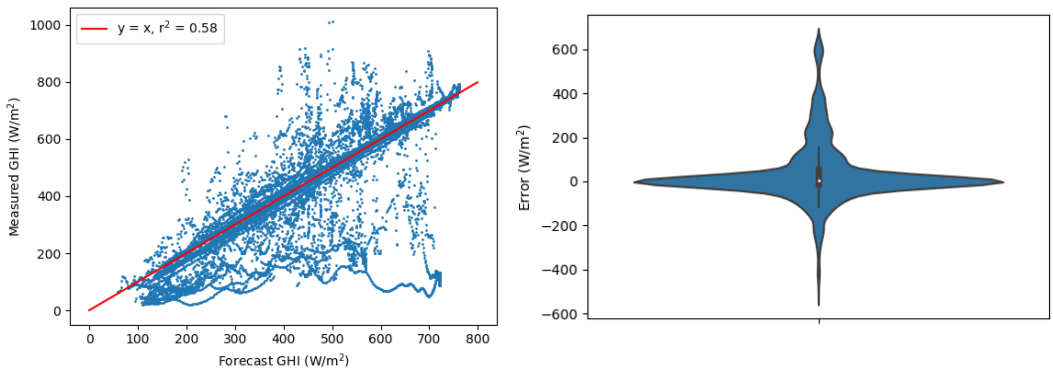

(a) Correlation **(b)** Error distribution

Figure 7. Correlation and distribution of three-hour forecast and measured GHI values

3.5. Radiation energy forecast validation

The energy received by radiations corresponds to the integration of GHI during time. Here, energy is forecasted each 3 hours at 5:00, 8:00, 11:00, 15:00, 17:00, 20:00, during 3 hours long. It means for instance a prediction at 5:00 of energy received from 5:00 to 8:00. **Figure 8** presents correlation between prediction using our model, and measures. The energy forecast has a high accuracy with coefficient of determination of 0.84. The energy forecast has better coefficient of determination r^2 than irradiance forecast, because energy is based on integration over time, so it reduce variations and rely more on the mean of irradiance.

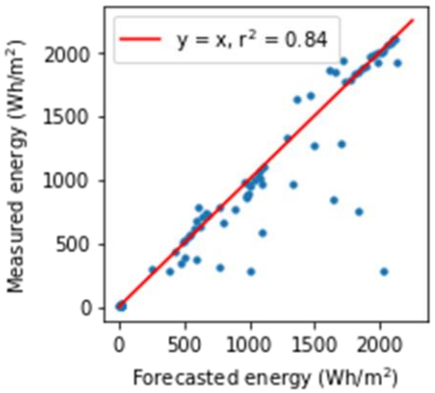

Figure 8.3 hours energy correlation

3.6. Long term forecast and energy management strategies

The cloudiness forecast is available for the next 8 days. Our modelling process has used the 0 hour data in order to have the more accurate cloudiness. The model prediction comparison and model validation has used the 3 hours forecast in order to validate the radiation and energy short term forecast. Now it is also possible to apply our model for the next 8 days, and then to have an energy production forecast for more than a week. It is not our aim in this study to evaluate the accuracy of weather forecast, but just to have an idea of uncertainties of model inputs such as cloudiness. **Figure 9** presents the comparison between forecast and measures. The red dashed line is the updated forecast, 1 day after the first forecast.

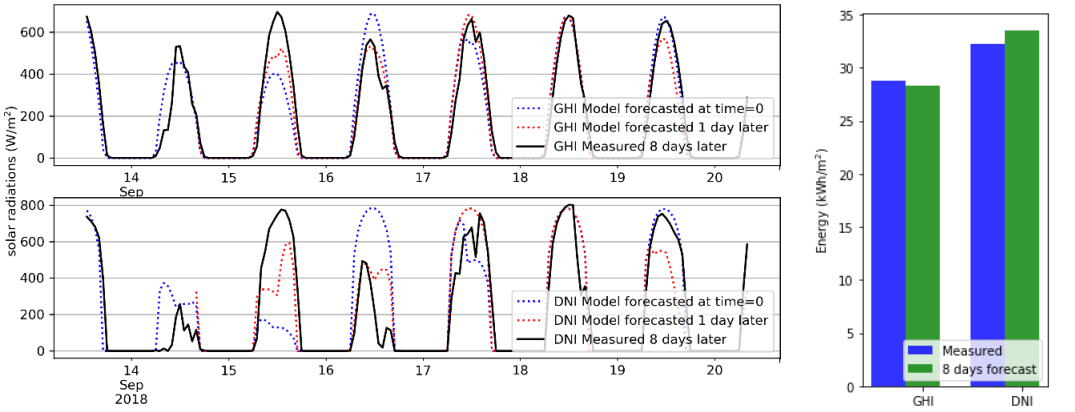

(a) Irradiances forecast compared to measures during 8 days **(b)** Energy comparison

Figure 9. 7 days forecast of GHI and DNI, comparison with measures

4. Conclusion

A methodology for PV energy forecast have been presented in this paper. It is based on irradiance forecasting model and cloudiness web service forecast. A first step was irradiance forecast model creation based on regression using past data. The second step is to simulate energy production based on irradiance model and cloudiness forecast on the next few hours. Our model has been compared with Perez model and Kasten and Czeplak model, and better results have been obtained using our hypothesis. Nevertheless, it has been applied using local measures, thus it can be inaccurate in another region, however, the methodology can be widely spread to any location. Only GHI data have been detailed, and the final results presents GHI as well as DNI. Then it has been shown in the validation step, that error from the irradiance forecast can be large due to weather forecast errors, but regarding energy production, the forecast is much more accurate. Thanks to the transposition model [21], PV production model is obtained. It is now possible to link it with consumption models and apply energy

management strategies to improve some performance indicators such as load matching of grid interaction [22]

5. References

[1] S. Wilbert *et al., Task 46: Best Practices for Solar Irradiance Measurements with Rotating Shadowband Irradiometers*. 2015.
[2] F. Kasten and G. Czeplak, "Solar and terrestrial radiation dependent on the amount and type of cloud," *Sol. Energy*, vol. 24, no. 2, pp. 177–189, Jan. 1980.
[3] R. Brinsfield, M. Yaramanoglu, and F. Wheaton, "Ground level solar radiation prediction model including cloud cover effects," *Sol. Energy*, vol. 33, no. 6, pp. 493–499, Jan. 1984.
[4] R. Perez, K. Moore, S. Wilcox, D. Renné, and A. Zelenka, "Forecasting solar radiation – Preliminary evaluation of an approach based upon the national forecast database," *Sol. Energy*, vol. 81, no. 6, pp. 809–812, Jun. 2007.
[5] D. Pepe, G. Bianchini, and A. Vicino, "Model estimation for solar generation forecasting using cloud cover data," *Sol. Energy*, vol. 157, pp. 1032–1046, Nov. 2017.
[6] D. Yang, P. Jirutitijaroen, and W. M. Walsh, "Hourly solar irradiance time series forecasting using cloud cover index," *Sol. Energy*, vol. 86, no. 12, pp. 3531–3543, Dec. 2012.
[7] M. Daneshyar, "Solar radiation statistics for Iran," *Sol. Energy*, vol. 21, no. 4, pp. 345–349, 1978.
[8] G. W. Paltridge and D. Proctor, "Monthly mean solar radiation statistics for Australia," *Sol. Energy*, vol. 18, no. 3, pp. 235–243, Jan. 1976.
[9] B. Haurwitz, "Insolation in relation to cloudiness and cloud density," *J. Meteorol.*, vol. 2, no. 3, pp. 154–166, Sep. 1945.
[10] V. Badescu, "Verification of some very simple clear and cloudy sky models to evaluate global solar irradiance," *Sol. Energy*, vol. 61, no. 4, pp. 251–264, Oct. 1997.
[11] Adnot J., Campana D., Gicquel R., and Bourges B, "Utilisation des courbes de frequence cumulees pour le calcul des installation solaires.," *Anal. Stat. Process. Meteorol. Appl. Energ. Sol. Lestienne R Ed*, pp. 9–40.
[12] L. Robledo and A. Soler, "Luminous efficacy of global solar radiation for clear skies," *Energy Convers. Manag.*, vol. 41, no. 16, pp. 1769–1779, Nov. 2000.
[13] Matthew J. Reno, Clifford W. Hansen, and Joshua S. Stein, "Global Horizontal Irradiance Clear Sky Models: Implementation and Analysis," Sandia National Laboratories, Albuquerque, New Mexico, Mar. 2012.
[14] E. G. Laue, "The measurement of solar spectral irradiance at different terrestrial elevations," *Sol. Energy*, vol. 13, no. 1, pp. 43–57, Apr. 1970.
[15] J. A. Ruiz-Arias and C. A. Gueymard, "Worldwide inter-comparison of clear-sky solar radiation models: Consensus-based review of direct and global irradiance components simulated at the earth surface," *Sol. Energy*, vol. 168, pp. 10–29, Jul. 2018.
[16] B. Haurwitz, "Insolation in relation to cloud type," *J. Meteorol.*, vol. 3, no. 4, pp. 123–124, Dec. 1946.
[17] H. C. Hottel, "A simple model for estimating the transmittance of direct solar radiation through clear atmospheres," *Sol. Energy*, vol. 18, no. 2, pp. 129–134, Jan. 1976.
[18] F. Kasten, "A Simple Parameterization of the Pyrheliometric Formula for Determining the Linke Turbidity Factor," *Meteorol. Rundsch.*, vol. 33, pp. 124–127, 1980.
[19] P. Ineichen and R. Perez, "A new airmass independent formulation for the Linke turbidity coefficient," *Sol. Energy*, vol. 73, no. 3, pp. 151–157, Sep. 2002.
[20] C. A. Gueymard, "Clear-sky irradiance predictions for solar resource mapping and large-scale applications: Improved validation methodology and detailed performance analysis of 18 broadband radiative models," *Sol. Energy*, vol. 86, no. 8, pp. 2145–2169, Aug. 2012.
[21] J. Hay and J. Davies, "Calculation of the solar radiation incident on an inclined surface.," *First Can. Sol. Radiat. Data Workshop Tor. Can.*, 1978.
[22] Salom, "Understanding net zero energy buildings: Evaluation of load matching and grid interaction indicators," *Build. Simul. Conf.*, 2011.